THE JOURNAL OF BIOLOGICAL CHEMISTRY VOL. 284, NO. 37, pp. 24797–24805, September 11, 2009

Bacterial-type Phosphoenolpyruvate Carboxylase (PEPC) Functions as a Catalytic and Regulatory Subunit of the Novel Class-2 PEPC Complex of Vascular Plants*[S]

Received for publication, May 19, 2009, and in revised form, July 13, 2009 Published, JBC Papers in Press, July 15, 2009, DOI 10.1074/jbc.M109.022863

Brendan O'Leary[‡], Srinath K. Rao[‡], Julia Kim[‡], and William C. Plaxton[‡§1]

From the Departments of [‡]Biology and [§]Biochemistry, Queen's University, Kingston, Ontario K7L 3N6, Canada

Phosphoenolpyruvate carboxylase (PEPC) is a tightly regulated anaplerotic enzyme situated at a major branch point of the plant C metabolism. Two distinct oligomeric classes of PEPC occur in the triglyceride-rich endosperm of developing castor oil seeds (COS). Class-1 PEPC is a typical homotetramer composed of identical 107-kDa plant-type PEPC (PTPC) subunits (encoded by *RcPpc3*), whereas the novel Class-2 PEPC 910-kDa hetero-octameric complex arises from a tight interaction between Class-1 PEPC and distantly related 118-kDa bacterial-type PEPC (BTPC) polypeptides (encoded by *RcPpc4*). Here, COS BTPC was expressed from full-length *RcPpc4* cDNA in *Escherichia coli* as an active PEPC that exhibited unusual properties relative to PTPCs, including a tendency to form large aggregates, enhanced thermal stability, a high $K_{m(PEP)}$, and insensitivity to metabolite effectors. A chimeric 900-kDa Class-2 PEPC hetero-octamer having a 1:1 stoichiometry of BTPC:PTPC subunits was isolated from a mixture of clarified extracts containing recombinant RcPPC4 and an *Arabidopsis thaliana* Class-1 PEPC (the PTPC, AtPPC3). The purified Class-2 PEPC exhibited biphasic PEP saturation kinetics with high and low affinity sites attributed to its AtPPC3 and RcPPC4 subunits, respectively. The RcPPC4 subunits: (i) catalyzed the majority of the Class-2 PEPC V_{max}, particularly in the presence of the inhibitor L-malate, and (ii) also functioned as Class-2 PEPC regulatory subunits by modulating PEP binding and catalytic potential of its AtPPC3 subunits. BTPCs appear to associate with PTPCs to form stable Class-2 PEPC complexes *in vivo* that are hypothesized to maintain high flux from PEP under physiological conditions that would otherwise inhibit Class-1 PEPCs.

Phosphoenolpyruvate (PEP)[2] carboxylase (PEPC; EC 4.1.1.31) is an important enzyme of plant C metabolism that catalyzes the irreversible β-carboxylation of phosphoenolpyruvate to yield oxaloacetate and P_i. This enzyme has been intensively studied with regards to its crucial role in catalyzing atmospheric CO_2 fixation in C_4 and crassulacean acid metabolism photosynthesis (1, 2). It also plays essential functions in bacteria and non-green plant cells, particularly the anaplerotic replenishment of tricarboxylic acid cycle intermediates withdrawn for biosynthesis and *N*-assimilation (3, 4). Most vascular plant PEPCs exist as a homotetrameric "dimer of dimer" structure composed of four identical 100–110-kDa subunits known as Class-1 PEPC. Class-1 PEPCs are subject to tight control by a combination of allosteric effectors and reversible phosphorylation at a conserved N-terminal seryl residue catalyzed by a dedicated Ca^{2+}-independent PEPC protein kinase and protein phosphatase type 2A (1–3). Allosteric activation by hexose phosphates and inhibition by malate have been routinely observed, whereas phosphorylation activates the enzyme by reducing its sensitivity to malate inhibition and simultaneously enhancing activation by hexose phosphates (1–3). Our understanding of the post-translational control of this enzyme has been further complicated by the discovery that Class-1 PEPC from germinated castor oil seeds (COS) is *in vivo* monoubiquitinated at a conserved Lys residue, resulting in increased $K_{m(PEP)}$ and enhanced sensitivity to metabolite effectors (5).

Plant PEPCs belong to small multigene families encoding closely related 100–110-kDa polypeptides containing the N-terminal seryl phosphorylation domain and critical C-terminal tetrapeptide QNTG that are distinguishing features of plant-type PEPCs (PTPCs) (2, 6). However, all plants examined to date also contain a single and enigmatic bacterial-type PEPC (BTPC) gene encoding a larger 116–118-kDa deduced polypeptide that: (i) exhibits low (<40%) sequence identity with PTPCs, (ii) lacks the N-terminal phosphorylation site typical of PTPCs, and (iii) contains a prokaryotic-like (R/K)NTG tetrapeptide at its C terminus (7–11). A functional BTPC enzyme has yet to be identified in vascular plants, although BTPC transcripts and genes have been well documented (7–9, 11, 12). Most insights into the occurrence, structure, and function of plant BTPC polypeptides have arisen from the biochemical characterization of unusual Class-2 PEPC hetero-oligomeric complexes from developing COS and unicellular green algae (10, 11, 13–18, 19), as well as an active recombinant BTPC from the green alga *Chlamydomonas reinhardtii* (20). During PEPC purification from the triglyceride-rich endosperm of developing COS, low and high M_r isoforms corresponding to a Class-1 PEPC and a novel hetero-octameric Class-2 PEPC were isolated and characterized (10). The COS Class-1 PEPC is a typical 410-kDa homotetramer composed of 107-kDa PTPC subunits

* This work was supported by grants from the Natural Sciences and Engineering Research Council of Canada (NSERC) and the Queen's Research Chairs program (to W. C. P.).

[S] The on-line version of this article (available at http://www.jbc.org) contains supplemental Table S1 and Figs. S1–S3.

[1] To whom correspondence should be addressed. Tel.: 613-533-6150; Fax: 613-533-6617; E-mail: plaxton@queensu.ca.

[2] The abbreviations used are: PEP, phosphoenolpyruvate; PEPC, PEP carboxylase; COS, castor oil seed; PTPC and BTPC, plant- and bacterial-type phosphoenolpyruvate carboxylase, respectively; FPLC, fast protein liquid chromatography; co-IP, co-immunopurification.

(encoded by *RcPpc3*; GenBank™ accession number EF634317) that are subject to reversible *in vivo* seryl phosphorylation in response to sucrose supply (10, 11, 13). By contrast, the purified Class-2 PEPC was characterized as a novel 681-kDa hetero-octamer arising from a tight interaction between Class-1 PEPC and unrelated 64-kDa polypeptides. Tryptic peptide sequencing revealed that the 64-kDa polypeptides matched the C-terminal half of deduced rice and *Arabidopsis* ~116-kDa BTPC polypeptides (10). Subsequent studies confirmed that the 64-kDa subunit was derived from a larger 118-kDa polypeptide via *in vitro* proteolysis, and that native COS Class-2 PEPC exists as a 910-kDa complex consisting of the Class-1 PEPC (RcPPC3) homotetrameric core tightly associated with four 118-kDa BTPC subunits (encoded by *RcPpc4*; GenBank accession number EF634318) that are *in vivo* phosphorylated at multiple sites (11, 14). Nevertheless, the interaction of RcPPC3 with truncated RcPPC4 polypeptides in the purified native Class-2 PEPC resulted in significant physical and kinetic differences between the COS Class-1 *versus* Class-2 PEPC that were remarkably analogous to the respective properties of Class-1 and Class-2 PEPCs from unicellular green algae. In particular, COS and green algal high M_r Class-2 PEPC complexes are largely desensitized to metabolite effectors and arise from a tight interaction between unrelated PTPC and BTPC polypeptides (10, 11, 13–18, 19). The combined data imply that Class-1 and Class-2 PEPC oligomers evolved in green algae prior to the evolution of vascular plants, with this feature being conserved as a key structure-function aspect of certain vascular plant PEPCs. Although no definitive physiological role has been established for Class-2 PEPC, it was hypothesized to support carbon flux to malate required for storage of lipid synthesis in developing COS (10). Our interest in COS PEPC was sparked by discoveries that: (i) exogenous L-malate supported maximal rates of fatty acid synthesis by purified leucoplasts from developing COS (21), and (ii) L-malate import from the cytosol into the leucoplast stroma is catalyzed by a malate/P_i translocator within the COS leucoplast envelope (22).

The deduced sequences of green algal and vascular plant BTPCs maintain conserved domains believed to be essential for PEPC catalytic activity (supplemental Fig. S1) (11, 20, 23). However, heterologous expression of BTPC from the model plant *Arabidopsis thaliana* in *Escherichia coli* yielded an inactive PEPC (8, 11), whereas all attempts to purify non-degraded native Class-2 PEPC from developing COS have been unsuccessful because of the extreme susceptibility of its BTPC subunits to *in vitro* truncation by an endogenous thiol endopeptidase (10, 11, 13). Thus, it remains uncertain whether vascular plant BTPCs exhibit PEPC activity, as is the case with green algal BTPCs (17, 19, 20), and/or function solely as a putative regulatory subunit within the Class-2 PEPC complex. The overall aim of the current study was to establish whether a non-proteolyzed preparation of the castor BTPC RcPPC4 exhibits catalytic activity or is capable of forming a functional Class-2 PEPC complex when incubated with Class-1 PEPC. Our results provide new insights into the functional significance of BTPC *versus* PTPC subunits of vascular plant Class-2 PEPCs, and demonstrate that the BTPC functions as a catalytic and regulatory subunit within the Class-2 PEPC complex.

EXPERIMENTAL PROCEDURES

Cloning, Transformation, and Heterologous Expression of Recombinant PEPCs—Full-length cDNAs encoding *RcPpc3* and *RcPpc4* were cloned as NdeI/XhoI and NdeI/NotI inserts, respectively, in a pET28b His tag vector (Novagen). The primer pairs used for *RcPpc3* were NdeI-3 forward 5′-AGCCATATGCAACCAAGGAATTTAGAGATG-3′, and XhoI-3 reverse 5′-CTCGAGTTAACCAGTGTTTTGTAGTCCAGC-3′. Primers for *RcPpc4* were NdeI-4 forward 5′-AGCCATATGACGGACACCACAGATGATATT-3′, and NotI-4 reverse 5′-GCGGCCGCTCAGCCTGTGTTCCTCATT-3′. The underlined nucleotide bases indicate restriction sites incorporated for directional cloning. Constructs used for producing recombinant His-tagged AtPPC3 and AtPPC4 were as previously described (11). PCR was performed with *Pfu* DNA polymerase (Fermentas) with full-length *RcPpc3* and *RcPpc4* cDNA as template, running 30 cycles of 95 °C for 30 s, 55 °C for 1 min, and 68 °C for 3 min. Both the vector and PCR product were digested with appropriate restriction enzymes, purified with a DNA gel extraction kit (MO BIO Laboratories), and directionally cloned overnight at room temperature with T4 DNA ligase (Fermentas). The ligated products were transformed in *E. coli* (BL21-CodonPlus (DE3)-RIL) (Stratagene) through electroporation and screened on LB plates containing 50 μg/ml kanamycin. The vector insert constructs were confirmed by restriction digestion of the isolated plasmid clones with Wizard Plus miniprep (Promega) and sequenced. Cells were cultured at 37 °C until an A_{600} of 0.6 was reached, incubated for 5 min at 4 °C, then induced for 3 h at 20 °C with 0.1 mM isopropyl β-D-1-thiogalactopyranoside. Recombinant expression was according to Thomas and Baneyx (24) for RcPPC4 and Kim *et al.* (25) for AtPPC3. The cultures were centrifuged and pellets were quick frozen in liquid N_2 and stored at −80 °C.

Purification of Recombinant RcPPC4, AtPPC3, and Class-2 PEPC—All procedures were performed at 4 °C, except column chromatography, which was conducted using an ÄKTA Fast Protein Liquid Chromatography (FPLC) system (GE Healthcare) at room temperature (25 °C). Buffer A contained 50 mM NaH_2PO_4 (pH 8.0), 300 mM NaCl, 15% (v/v) glycerol, and 1 mM dithiothreitol. Buffer B contained 100 mM KH_2PO_4 (pH 8.0), 1 mM EDTA, 2 mM $MgCl_2$, 5 mM malate, 15% (v/v) glycerol, and 1 mM dithiothreitol. *E. coli* cells (16 g) containing recombinant RcPPC4 were thawed in 60 ml of buffer A and lysed by passage through a French press at 20,000 p.s.i. After centrifugation the supernatant was loaded at 1 ml/min onto a column (1.6 × 10 cm) of PrepEase™ His-tagged High Yield Purification Ni^{2+}-affinity resin (U. S. Biochemical Corp.). The column was washed with buffer A until the A_{280} approached baseline, then eluted with buffer A containing 150 mM imidazole. Pooled peak fractions were concentrated to 2 ml with an Amicon Ultra-15 centrifugal filter unit (100-kDa cutoff), then loaded at 0.3 ml/min onto a Superdex-200 HR 16/50 column equilibrated with buffer B. Pooled peak fractions were concentrated as above to <1 ml and stored at −20 °C in 50% (v/v) glycerol. The purified BTPC lost about 35% of its PEPC activity after 2 weeks of storage.

For simultaneous purification of recombinant Class-1 PEPC (AtPPC3) and chimeric Class-2 PEPC (containing recombinant

RcPPC4 and AtPPC3), freshly prepared clarified extracts from 3 g of AtPPC3- and 6 g of RcPPC4-expressing *E. coli* cells were immediately mixed and subjected to PrepEase™ Ni^{2+}-affinity and Superdex-200 FPLC as described above. Pooled Class-1 and Class-2 PEPC peak fractions from the Superdex 200 column (Fig. 1*B*) were separately concentrated as above to 250 μl and subjected to FPLC on a calibrated Superose-6 10/300 GL column (10) at 0.25 ml/min. Pooled peak fractions were concentrated as above to <1 ml and stored at −20 °C in 50% (v/v) glycerol. The PEPC activity of the final Class-1 and Class-2 PEPC preparations was stable for at least 2 months when stored under these conditions.

Electrophoresis and Immunoblotting—SDS and non-denaturing PAGE using a Bio-Rad Protean III mini-gel system, subunit and native M_r estimates via SDS- and non-denaturing PAGE, in-gel PEPC activity staining, and immunoblotting were as described previously (10). Antigenic polypeptides were visualized using an alkaline phosphatase-conjugated secondary antibody and chromogenic detection (26). All immunoblot results were replicated a minimum of three times with representative results shown in the figures. Rabbit anti-(native RcPPC3) IgG was raised against homogeneous Class-1 PEPC from developing COS as described previously (11). Rabbit antiserum was also raised against homogeneous recombinant RcPPC4 that had been dialyzed overnight in P_i-buffered saline and emulsified 1:1 in TiterMax Gold adjuvant (CytRx Corp.). Following collection of preimmune serum, 200 μg of RcPPC4 was injected subcutaneously into a rabbit, and a 150-μg booster injection was administered 28 days later. At 9 days after the final injection, blood was collected in Vacutainer tubes (Becton Dickinson) by cardiac puncture. Clotted cells were removed by centrifugation and the immune serum frozen in liquid N_2 and stored at −80 °C in 0.04% (w/v) NaN_3. For immunoblotting, anti-RcPPC4-IgG was affinity purified against 500 μg of nitrocellulose-bound homogeneous recombinant RcPPC4 as previously described (26).

Co-immunopurification—This was performed as previously described (14). A clarified extract from 5 g of stage V (mid-cotyledon) developing COS endosperm was eluted at 0.5 ml/min through a column containing 1.5 mg of protein A-purified anti-RcPPC4-IgG that had been covalently coupled to 1 ml of AminoLink plus gel (Pierce Chemicals) as per the manufacturer's instructions. After washing non-bound proteins from the column with P_i-buffered saline containing 10 μl/ml ProteCEASE-100 (G-Biosciences), absorbed proteins were eluted with 100 mM glycine HCl (pH 2.8), neutralized with unbuffered Tris, and concentrated to approximately 1 mg/ml prior to analysis of their polypeptide composition by SDS-PAGE and immunoblotting.

Enzyme and Protein Assays and Kinetic Studies—The PEPC activity was assayed at 25 °C by following NADH oxidation at 340 nm in a final volume of 200 μl using a Spectramax Plus microplate reader (Molecular Devices) and the following optimized assay mixture: 50 mm Hepes-KOH (pH 8.0) containing 10% (v/v) glycerol, 10 mM PEP, 5 mM $KHCO_3$, 10 mM $MgCl_2$, 2 mM dithiothreitol, 0.15 mM NADH, and 5 units/ml of desalted porcine muscle malate dehydrogenase. One unit of PEPC is defined as the amount of enzyme resulting in the production of 1 μmol of oxaloacetate/min. Protein concentrations were determined by the Coomassie Blue G-250 dye binding method using bovine γ-globulin as the protein standard (10). Apparent V_{max} and $K_{m(PEP)}$, and IC_{50} values (inhibitor concentration producing 50% inhibition of PEPC activity) were routinely calculated using a nonlinear least square regression computer program (27). For the chimeric Class-2 PEPC, PEP saturation data were fitted to both single and two active site models using nonlinear regression analysis software (SigmaPlot Version 10.0 (SPSS Inc.)) as previously described (17). All kinetic parameters represent means of at least four separate determinations and are reproducible to within ±15% (S.E.) of the mean value unless otherwise noted. Stock solutions of all metabolites were made equimolar with $MgCl_2$ and adjusted to pH 7.0.

Statistics—Data were analyzed using the Student's *t* test, and deemed significant at $p < 0.05$.

RESULTS

Heterologous Expression, Purification, and Immunological Characterization of the Bacterial-type PEP Carboxylase RcPPC4 from Developing Castor Oil Seeds

Full-length RcPPC4-encoding cDNA (11) was subcloned into a pET28b expression vector with an N-terminal His_6 tag and transformed into several expression strains. Optimal results were obtained with *E. coli* BL21(DE3) in which RcPPC4 was expressed as an active PEPC in the soluble fraction. About 1 mg of RcPPC4 was purified 250-fold to apparent homogeneity and a final specific PEPC activity of 27 units/mg by a combination of Ni^{2+} affinity and Superdex-200 FPLC (Figs. 1*A* and 2*A*, supplemental Table S1). The tendency of RcPPC4 to form large aggregates was reflected by its consistent elution in the void volume during Superdex-200 or Superose-6 gel filtration FPLC (molecular mass > 2 MDa), and efficient precipitation with a relatively low concentration (5%, w/v) of polyethylene glycol 8,000 (Fig. 1*A* and results not shown). The final RcPPC4 preparation proved difficult to store as it slowly lost activity when maintained at −20 °C in 50% (v/v) glycerol, and was completely inactivated when rapidly thawed after freezing in liquid N_2. After digestion with the endopeptidase thrombin to remove the His_6 tag used for purification, RcPPC4 was cleaved into approximately 64- and 50-kDa polypeptides (supplemental Fig. S2). This parallels the well documented susceptibility of the native RcPPC4 to rapid proteolysis to similarly sized polypeptides by an endogenous thiol endopeptidase during incubation of clarified COS extracts on ice, or native Class-2 PEPC purification from developing COS (supplemental Fig. S2) (10, 11, 13). Thus, all subsequent studies were conducted using His_6-tagged RcPPC4.

Rabbit immunization with purified RcPPC4 led to the production of affinity purified anti-RcPPC4-IgG that cross-reacted with as little as 10 ng of the corresponding antigen and was monospecific for 118-kDa RcPPC4 polypeptides on immunoblots of developing COS extracts (Fig. 2*B*). By contrast, immunoblots of RcPPC4 failed to cross-react with anti-RcPPC3-IgG and vice versa (Fig. 2, *B*, *D*, and *E*). This corroborates the well documented sequence and immunological distinctiveness between vascular plant and green algal BTPCs and PTPCs (8,

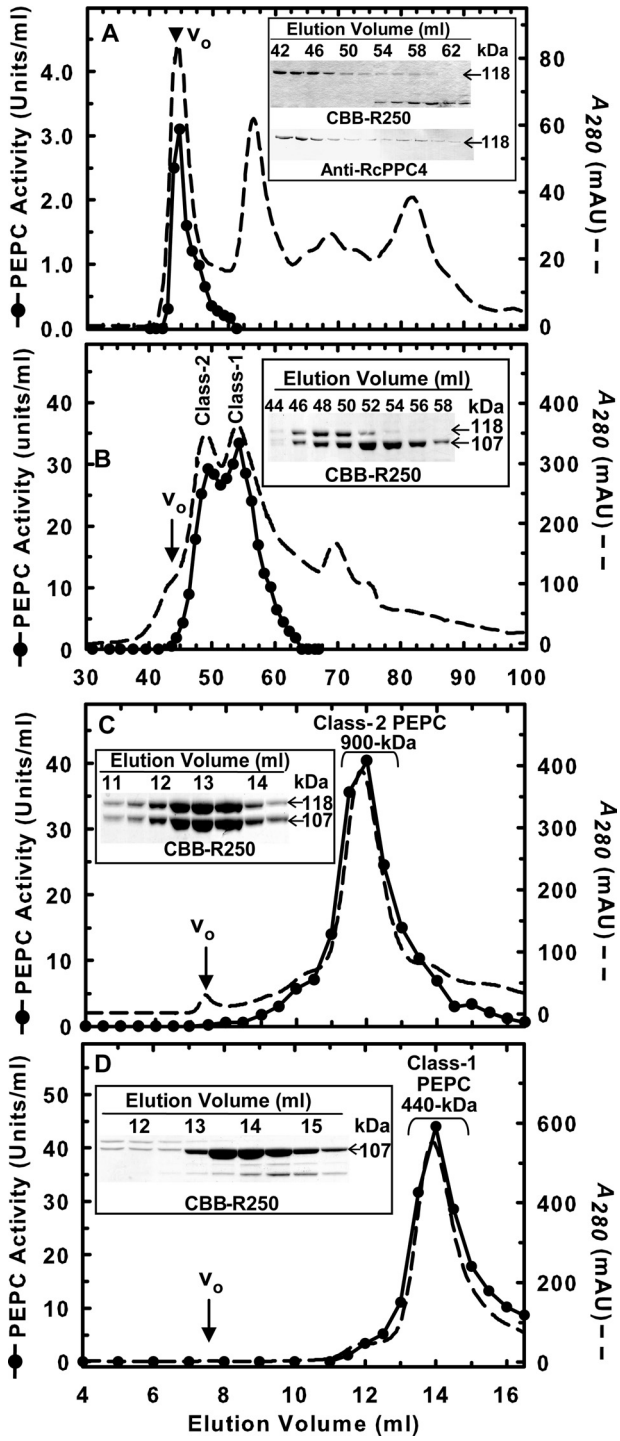

FIGURE 1. **Purification of recombinant RcPPC4, AtPPC3, and a chimeric Class-2 PEPC by gel filtration FPLC.** *A*, Superdex-200 HR 16/50 elution profile for recombinant RcPPC4. *B*, Superdex-200 HR 16/50 elution profile indicating the position of Class-2 and Class-1 PEPCs obtained from a mixture of recombinant RcPPC4 and AtPPC3. Fractions eluting at 46–50 and 54–59 ml were pooled to enrich Class-2 and Class-1 PEPC, respectively. *C* and *D*, Superose-6 10/300 GL elution profiles of the chimeric Class-2 PEPC (RcPPC4 + AtPPC3) hetero-octamer (*C*) and Class-1 PEPC (AtPPC3) homotetramer (*D*). *Insets*, aliquots (*A*, 7-μl each; *B–D*, 2-μl each) from various fractions were subjected to SDS-PAGE followed by protein staining with Coomassie Brilliant Blue R-250 (*CBB-R250*) (*A–D*), or immunoblotting with anti-RcPPC4-IgG (*A*). V_0 denotes the void volume.

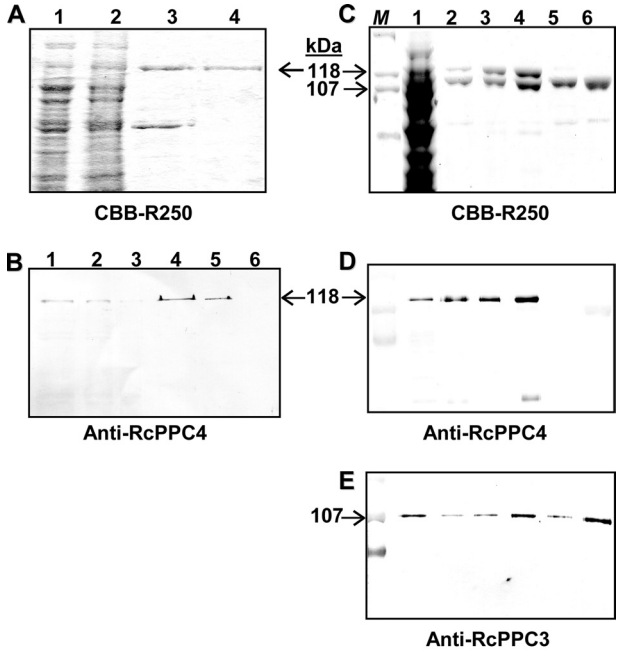

FIGURE 2. **SDS-PAGE and immunoblot analysis of purified recombinant PEPC isoforms.** *A*, SDS-PAGE followed by Coomassie Brilliant Blue (*CBB*) R-250 staining was performed on various fractions obtained during the purification of the recombinant BTPC, RcPPC4. *Lanes 1–4*, respectively, contain 20, 20, 10, and 2.5 μg of the clarified soluble extract, corresponding insoluble (inclusion body) fraction, pooled PrepEase™ Ni^{2+}-affinity fractions, and pooled Superdex-200 fractions. *B*, various amounts of a clarified extract from stage V (mid-cotyledon) developing COS and purified recombinant RcPPC4 were subjected to SDS-PAGE followed by immunoblotting with a 1:250 dilution of affinity purified anti-RcPPC4-IgG. *Lanes 1–3*, respectively, contain 10, 5, and 2.5 μg of the clarified COS extract, whereas *lanes 4–6* contain 25, 10, and 2.5 ng of pure RcPPC4. *C-E*, aliquots from various stages of concurrent Class-2 PEPC (RcPPC4 + AtPPC3) and Class-1 PEPC (AtPPC3) purification were subjected to SDS-PAGE followed by staining with Coomassie Brilliant Blue R-250 (*C*), and immunoblotting with anti-RcPPC4-IgG (*D*) or anti-RcPPC3-IgG (*E*). *Lane 1* of *panels C–E*, respectively, correspond to 60, 0.2, and 3 μg of the combined clarified *E. coli* extracts containing soluble recombinant AtPPC3 and RcPPC4. Likewise, *lanes 2* of *panels C–E*, respectively, contain 5, 0.3, and 1.5 μg of the pooled Ni^{2+}-affinity column fractions; *lanes 3* and *4* of *panels C–E*, respectively, contain 2, 0.1, and 0.02 μg of pooled chimeric Class-2 PEPC fractions from the Superdex-200 (*lane 3*) and Superose-6 (*lane 4*) columns; *lanes 5* and *6*, respectively, contain 2, 0.1, and 0.01 μg of the pooled Class-1 PEPC AtPPC3 fractions from the Superdex-200 (*lane 5*) and Superose-6 (*lane 6*) columns. *M* denotes various prestained SDS-PAGE M_r standard.

10, 11, 15, 17, 19, 20). Nevertheless, RcPPC4 quantitatively co-immunopurified with a similar amount of RcPPC3 following elution of developing COS extracts through an anti-RcPPC4-IgG immunoaffinity column (Fig. 3*A*). Non-denaturing PAGE followed by in-gel PEPC activity staining and parallel spectrophotometric PEPC activity assays established that 100% of Class-2 PEPC corresponding to 48 ± 6% (mean ± S.E., $n = 3$) of the total PEPC activity present in the initial clarified COS extract was absorbed by the anti-RcPPC4-IgG co-immunopurification (co-IP) column (Fig. 3*B*). By contrast, the Class-1 PEPC (RcPPC3) homotetramer was eluted in the corresponding flow-through/unbound fractions.

Recombinant RcPPC4 Forms Class-2 PEPC When Combined with Class-1 PEPCs

Non-denaturing PAGE of recombinant RcPPC4 failed to produce a PEPC activity staining band, but generated an anti-RcPPC4-IgG immunoreactive smear that reflects its propensity to aggregate into insoluble precipitates (Fig. 4, *A* and *B*). However, when preincubated with homogenous native Class-1

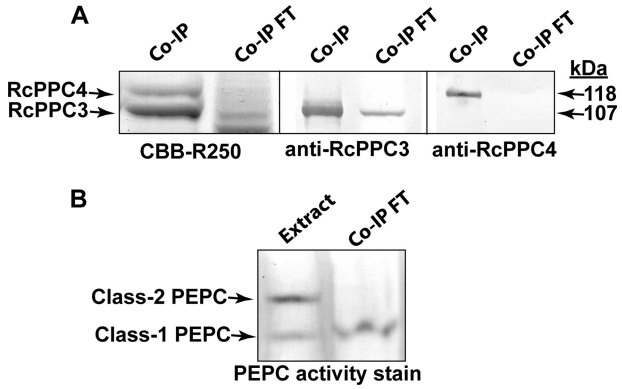

FIGURE 3. **Co-immunopurification of the native Class-2 PEPC complex from developing COS endosperm by anti-RcPPC4-IgG immunoaffinity chromatography.** A clarified extract from 5 g of stage V (mid-cotyledon) developing COS endosperm was precleared with a preimmune serum protein column (14) prior to elution through the anti-RcPPC4-IgG column. *A*, bound proteins eluted from the anti-RcPPC4-IgG column with Gly-HCl (pH 2.8) (*co-IP*) and pooled unbound flow-through fractions (*Co-IP FT*) were analyzed by 10% SDS-PAGE followed by Coomassie Brilliant Blue (*CBB*) R-250 staining or immunoblotting with anti-(RcPPC3 or RcPPC4)-IgG. Co-IP and co-IP flow-through lanes, respectively, contained 8 and 40 μg of protein (for Coomassie Brilliant Blue R-250 staining) or 1 and 20 μg of protein (for immunoblotting). *B*, the PEPC isoforms present in the initial clarified extract (*Extract*) and pooled co-IP flow-through fractions were visualized by 5% non-denaturing PAGE followed by in-gel PEPC activity staining (3 milliunits/lane).

PEPC from developing COS and analyzed by non-denaturing PAGE, recombinant RcPPC4 produced a Class-2 PEPC activity staining band composed of immunoreactive RcPPC3 and RcPPC4 polypeptides that co-migrated with the native 910-kDa Class-2 PEPC from stage III developing COS (Fig. 4, *A–C*). Above a 1:1 stoichiometric ratio of recombinant RcPPC4:native RcPPC3, only modest gains in the proportion of Class-2 PEPC relative to Class-1 PEPC were obtained, with the bulk of RcPPC4 visualized as an immunoreactive smear (Fig. 4, *A* and *B*). Non-denaturing PAGE followed by in-gel PEPC activity staining also established that RcPPC4 was associated into Class-2 PEPC complexes when preincubated with purified native Class-1 PEPCs from germinating COS (5), *Arabidopsis* and *Brassica napus* suspension cell cultures (28, 29), and ripened banana fruit (30) (Fig. 4*D*). Slower migrating, higher M_r PEPC isoforms were also evident on the non-denaturing gels when the recombinant RcPPC4 was mixed with several Class-1 PEPCs (Fig. 4*D*). This is reminiscent of native Class-2 PEPC isoforms from the green alga *Selenastrum minutum*, which exists as three large but kinetically similar protein complexes containing various stoichiometric ratios of BTPC and PTPC polypeptides (15, 17, 18).

Purification of a Non-proteolyzed Chimeric Class-2 PEPC from Recombinant RcPPC4 and AtPPC3

Heterologous expression of recombinant PEPCs in *E. coli* BL21(DE3) was also attempted with RcPPC3 and AtPPC4 (*Arabidopsis* BTPC ortholog; 79% identity). Both failed to yield soluble, active PEPC under a variety of induction conditions using constructs with and without an N-terminal His_6 tag. Similarly, co-expression of either AtPPC3 with AtPPC4, or RcPPC3 with RcPPC4 using the pETDuet-1 vector system (Novagen) did not result in active Class-2 PEPCs (results not shown). However, AtPPC3 (*Arabidopsis* PTPC ortholog of RcPPC3; 89% identity)

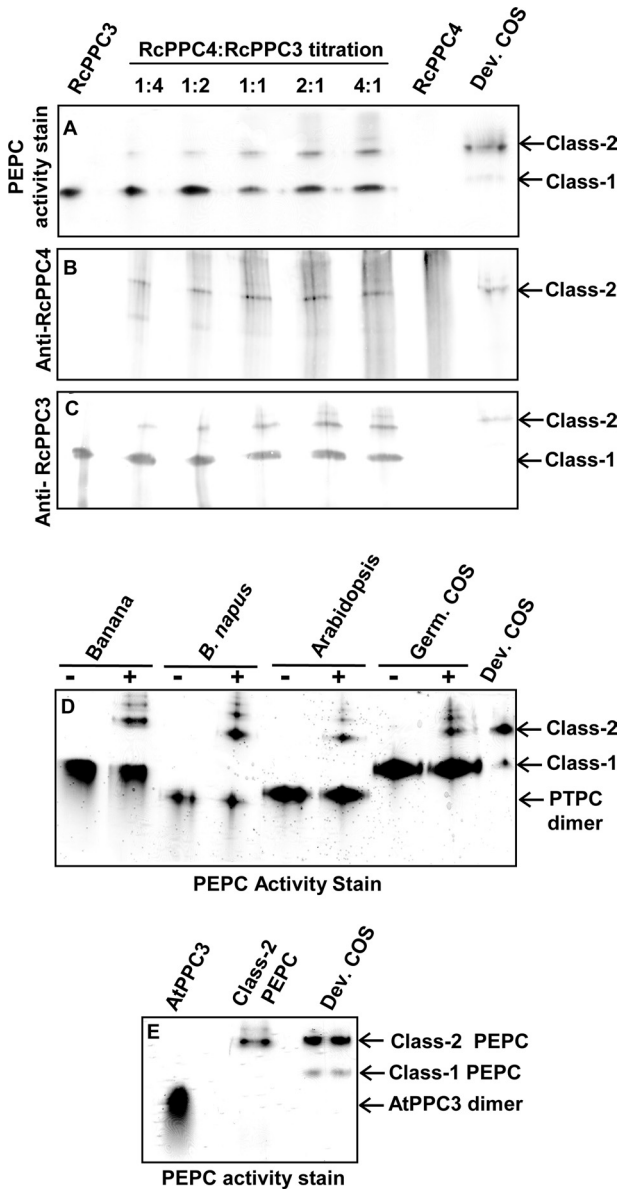

FIGURE 4. **Non-denaturing PAGE analysis of *in vitro* Class-2 PEPC formation.** *A–D*, homogeneous native Class-1 PEPCs were incubated with the purified recombinant RcPPC4 for 1 h at 25 °C in 50 mM Hepes-KOH, pH 7.7 (final volume = 25-μl). The mixtures were subjected to non-denaturing PAGE (7% separating gel) and in-gel PEPC activity staining (*A* and *D*) or immunoblotting with anti-RcPPC4-IgG (*B*) or anti-RcPPC3-IgG (*C*). *A–C*, various amounts of RcPPC4 were incubated with homogeneous Class-1 PEPC from developing COS (RcPPC3; 5.5 μg). *Lanes 1–6* contain 2.5 μg of RcPPC3 and a proportional amount of RcPPC4; *lane 7* contains 5 μg of RcPPC4; *lane 8* contains 20 μg of clarified extract from stage III (heart-shaped embryo) COS, wherein Class-2 PEPC is the predominant isoform (10). *D*, purified native Class-1 PEPCs from various vascular plant sources (10 milliunits each) were incubated with (+) or without (−) 10 milliunits of purified RcPPC4 as described above. The designations are as follows: *Banana*, banana fruit PEPC (30); *B. napus*, PEPC from P_i-starved *B. napus* suspension cell cultures (28); *Arabidopsis*, AtPPC1 from P_i-starved *Arabidopsis* suspension cells (29); *Germ. COS*, monoubiquitinated Class-1 PEPC (RcPPC3) from germinating COS (5). *Dev. COS* denotes 10 milliunits of PEPC activity from a clarified extract prepared from stage V (mid-cotyledon) developing COS endosperm. *E*, non-denaturing PAGE followed by in-gel PEPC activity staining was performed on purified recombinant AtPPC3 and chimeric Class-2 PEPC together with a clarified extract from stage V developing COS (4 milliunits/lane).

was readily expressed as an active, soluble Class-1 PEPC composed of 107-kDa subunits as previously described (11). Freshly prepared, clarified extracts from *E. coli* expressing RcPPC4 and

TABLE 1
Purification of recombinant Class-1 and -2 PEPCs from combined clarified extracts originating from 3 g of AtPPC3- and 6 g of RcPPC4-expressing *E. coli* cells

Step	Activity	Protein	Specific activity	Purification	Yield
	units	*mg*	*units/mg*	*-fold*	*%*
Clarified extracts					
AtPPC3	164	540	0.30		
RcPPC4	88	1458	0.060		
Combined extracts	270	2140	0.13	1	100
Ni^{2+}-affinity FPLC	256	60	4.3	34	95
Superdex-200 FPLC					
Class-1 PEPC	71.3	12.9	5.5	44	26
Class-2 PEPC	87.7	7.8	11.2	89	32
Superose-6 FPLC					
Class-1 PEPC	66.6	4.4	15.1	106	25
Class-2 PEPC	60.5	2.4	25.2	152	22

AtPPC3 were mixed at 25 °C and 2.4 mg of a chimeric Class-2 PEPC complex subsequently purified about 150-fold to apparent homogeneity by a combination of Ni^{2+} affinity, and sequential Superdex-200 and Superose-6 gel filtration FPLC (Figs. 1, *B* and *C*, and 2, *C-E*, Table 1). The Class-2 PEPC activity peak obtained during Superdex-200 or Superose-6 FPLC co-eluted with a 1:1 ratio of protein-staining RcPPC4 and AtPPC3 subunits (Fig. 1, *B* and *C*). The native M_r of the Class-2 PEPC as estimated by FPLC on a calibrated Superose-6 column was 900 ± 15 kDa (mean ± S.E., $n = 3$) (Fig. 1*C*), which corroborates its co-migration with the 910-kDa native Class-2 PEPC from stage III developing COS during non-denaturing PAGE (Fig. 4*E*). Thus, the purified chimeric Class-2 PEPC exists as a hetero-octamer composed of an equivalent ratio of non-proteolyzed 118-kDa RcPPC4 and 107-kDa AtPPC3 subunits. Class-1 PEPC was not detected in the final Class-2 PEPC preparation (Fig. 4*E*). Moreover: (i) the Class-2 PEPC complex did not dissociate over time as no Class-1 PEPC was visualized in subsequent PEPC activity stained non-denaturing gels (results not shown), and (ii) throughout several purification trials the RcPPC4 subunits were quantitatively bound by AtPPC3 to form the hetero-octameric Class-2 PEPC (Fig. 1, *B* and *C*). About 4 mg of excess AtPPC3 was simultaneously purified to a final specific activity of 15.1 units/mg (Figs. 1, *B* and *D*, and 2, *C* and *E*, Table 1). The native M_r of AtPPC3 as estimated during FPLC on the calibrated Superose-6 column was 440 ± 5 kDa (mean ± S.E., $n = 3$) (Fig. 1*D*), indicating that it exists as a typical Class-1 PEPC homotetramer composed of identical 107-kDa subunits. However, AtPPC3 appeared to dissociate into active dimers upon non-denaturing PAGE (Fig. 4*E*).

The three recombinant PEPC isoforms differed in their thermal stability (Fig. 5). Similar to Class-1 PEPC homotetramers from developing COS and green algae (10, 15–17), purified AtPPC3 was relatively heat-labile, losing over 95% of its activity when preincubated at 50 °C for 3 min. By contrast, the RcPPC4 was comparatively heat-stable, whereas the chimeric Class-2 PEPC exhibited an intermediate thermal stability (Fig. 5). This is consistent with previous studies documenting the enhanced thermal stability of green algal and vascular plant Class-2 PEPCs, relative to the corresponding Class-1 PEPC isoform (10, 15–17).

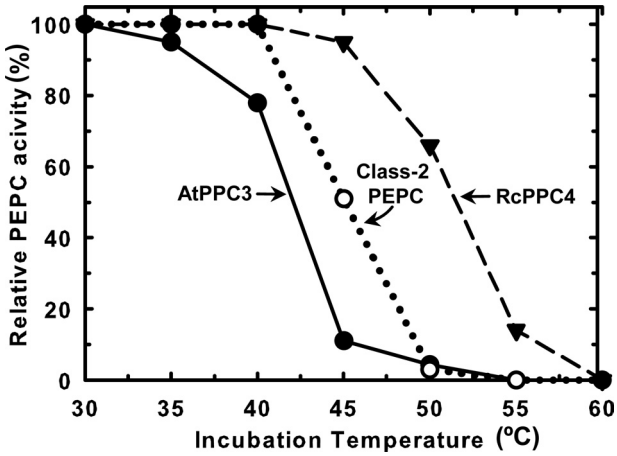

FIGURE 5. **Heat denaturation profiles of recombinant PEPCs.** Aliquots of purified PEPCs were incubated at a given temperature for 3 min. The samples were cooled on ice for 3 min, and residual PEPC activity determined at 25 °C. Activities are expressed relative to the corresponding control set at 100% (equivalent to 15, 27, and 25 units/mg of AtPPC3, RcPPC4, and chimeric Class-2 PEPC, respectively). All values represent the means of three different experiments and are reproducible to within ±10% of the mean value.

Kinetic Properties

Effect of pH and Metal Cofactor Requirements—Similar to other plant PEPCs (1), the activity of the purified recombinant AtPPC3, RcPPC4, and chimeric Class-2 PEPC: (i) displayed a broad pH profile with optimal activity occurring in the pH 8.0–8.5 range (supplemental Fig. S3), and (ii) was absolutely dependent upon the presence of a bivalent metal cation cofactor, specifically Mg^{2+} or Mn^{2+}. Metal ion requirements of RcPPC4 were investigated in more detail. It exhibited a 4-fold higher specific activity with saturating (10 mM) Mg^{2+} relative to Mn^{2+}, and a $K_{m(Mg^{2+})}$ value of 0.10 ± 0.01 mM.

PEP Saturation Kinetics—RcPPC4 and AtPPC3 both displayed hyperbolic PEP saturation kinetics at pH 8.0 and physiological pH (7.3) (Table 2). However, the apparent $K_{m(PEP)}$ value of RcPPC4 at both pH values was about an order of magnitude greater than that of AtPPC3 whose $K_{m(PEP)}$ of approximately 70 μM is typical for a C_3 plant PEPC (1). PEP binding to the chimeric Class-2 PEPC was analyzed by fitting PEP saturation data to a single catalytic site Michaelis-Menten model or to a two-catalytic site Michaelian model using non-linear regression. The fit to the two-catalytic site model yielded a higher probability ($p < 0.001$). The biphasic PEP saturation kinetics of the Class-2 PEPC was visualized by Eadie-Hofstee plots of the kinetic data (Fig. 6*A*). The theoretical plot of the two-site model (*solid line*) fit the experimental points with a correlation coefficient of 0.99, whereas the plot obtained assuming a single catalytic site (*dashed line*) has a far lower correlation coefficient of 0.87. These results indicate that the RcPPC4 and AtPPC3 subunits are both catalytically active within the Class-2 PEPC, as previously inferred for a green algal Class-2 PEPC (17). The apparent $K_{m(PEP)}$ values for the two sites differed by approximately 15-fold with the high K_m site (attributed to RcPPC4) displayed a 5-fold higher $V_{max(app)}$ at both pH 8.0 and 7.3 (Table 2). Because the RcPPC4 and AtPPC3 subunits occur in a 1:1 stoichiometric ratio within the Class-2 complex (Figs. 1*C* and 2*C*), their relative catalytic efficiencies were compared as $V_{max(app)}/K_{m(PEP)}$ (Table 2). The low K_m site (attributed to AtPPC3)

TABLE 2

PEP saturation kinetics of recombinant PEPCs

The standard spectrophotometric assay was used except that the PEP concentration was varied. Apparent V_{max} and $K_{m(PEP)}$ values represent the mean of four separate determinations and are reproducible within ±15% (S.E.) of the mean, with the exception of the values for the Class-2 PEPC low K_m site, which have an error of approximately ±30% (S.E.).

Assay	Class-1 PEPC (AtPPC3)			RcPPC4			Class-2 PEPC (AtPPC3 + RcPPC4)					
pH	V_{max}	K_m	V_{max}/K_m	V_{max}	K_m	V_{max}/K_m	V_{max1}[a]	K_m1	V_{max1}/K_{m1}	V_{max2}[a]	K_{m2}	V_{max2}/K_{m2}
	units/mg	μM	*units/mg* μM^{-1}	*units/mg*	μM	*units/mg* μM^{-1}	*units/mg*	μM	*units/mg* μM^{-1}	*units/mg*	μM	*units/mg* μM^{-1}
7.3	15.4	77	0.20	26.7	840	0.032	4.0	38	0.11	21.4	580	0.037
8.0	15.1	65	0.23	28.0	870	0.032	4.5	34	0.13	20.7	560	0.037

[a] V_{max1} and V_{max2} values are listed as units/mg of Class-2 PEPC. As AtPPC3 and RcPPC4 occur in a 1:1 stoichiometric ratio in the Class-2 PEPC, the $V_{max(app)}$ of individual AtPPC3 and RcPPC4 subunits within the Class-2 PEPC complex can be estimated by doubling V_{max1} and V_{max2}, respectively.

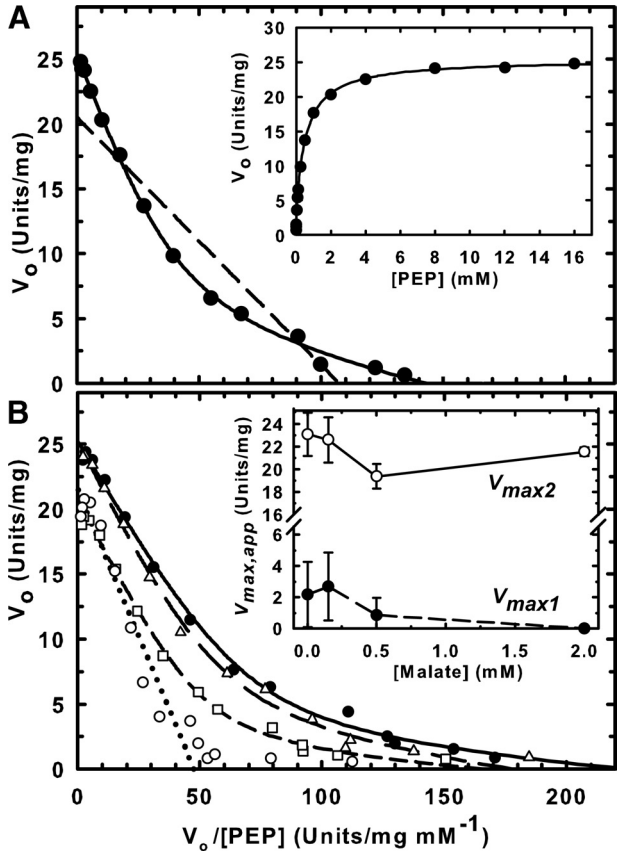

FIGURE 6. **Analysis of the biphasic PEP saturation kinetics of a chimeric Class-2 PEPC.** *A*, PEP saturation curves were determined at pH 7.3 and fitted to either a single catalytic site Michaelis-Menten model (*dashed line*) or a biphasic model with two distinct catalytic sites (*solid line*) and plotted as Eadie-Hofstee linearizations. *Inset*, plot of the reaction rate *versus* PEP concentration. *B*, PEP saturation curves were determined at pH 7.0 in the presence of 0 (●), 0.2 (Δ), 0.5 (□), and 2 mM (○) malate and analyzed as above. *Inset*, relationship between $V_{max(app)}$ values and malate concentration. V_{max1} (●) and V_{max2} (○) correspond to the $V_{max(app)}$ values obtained for the low (AtPPC3) and high (RcPPC4) $K_{m(PEP)}$ sites, respectively, as discussed in the text. All data represent the mean ± S.E. of four separate determinations.

was 3- and 3.5-fold more efficient at pH 7.3 and 8.0, respectively.

Metabolic Effectors

A variety of compounds were tested as possible effectors of the three recombinant PEPC isoforms at pH 8.0 and 7.0 with subsaturating PEP (0.2 mM). At pH 8.0 there was a negligible effect (±15% of the control rate) by glucose 6-P, fructose 6-P, glycerol 3-P, malate, Asp, or Glu (5 mM each) on the activity of AtPPC3, RcPPC4, or the chimeric Class-2 PEPC. However, as

TABLE 3

Influence of selected metabolites on the activity of recombinant PEPCs

The PEPC activity was determined at pH 7.0 with subsaturating PEP (0.2 mM) in the presence of each effector at 2 mM. Activities are expressed relative to the respective control determined in the absence of any additions and set at 100%. Shown in parentheses are IC_{50}(malate, Asp) values determined at pH 7.0 with 0.2 mM PEP. All values represent the mean of four separate determinations and are reproducible within ± 10% (S.E.) of the mean value.

Addition	Relative activity		
	Class-1 PEPC AtPPC3	RcPPC4	Class-2 PEPC AtPPC3/RcPPC4
Glc-6-P	191	93	121
Glc-1-P	171	95	114
Fru-6-P	188	99	119
Glycerol 3-P	185	98	120
Malate	8.5 (0.16)[a]	84 (11)[a]	20 (0.56)[a]
Aspartate	36 (0.97)[a]	98 (33)[a]	63 (2.8)[a]

[a] IC_{50} values represent inhibitor concentration (mM) yielding 50% inhibition of PEPC activity.

previously documented for a variety of plant Class-1 PEPCs including the developing COS Class-1 PEPC (RcPPC3) (1, 10, 13), AtPPC3 was significantly activated by hexose monophosphates and glycerol 3-P, and potently inhibited by malate and Asp when assayed at pH 7.0 (Table 3). Interestingly, RcPPC4 activity was unresponsive (±10% of the control rate) to 25 mM Glc-6-P, Fru-6-P, or glycerol 3-P, whereas its IC_{50} values for Asp and malate were, respectively, 34- and 69-fold greater than those obtained for AtPPC3 under identical assay conditions (Table 3). The following metabolites had no detectable effect on RcPPC4 activity (tested at pH 7.0 and subsaturating PEP): 50 mM Gly; citrate, isocitrate, ribose 5-P, gluconate 6-P, succinate, fumarate, pyruvate, acetate, fructose 1,6-P_2, ATP, ADP, AMP, PP_i, P_i, Gln, Asn, Ser, Arg, Ala, and Cys (5 mM each); 1 mM shikimic acid; dihydroxyacetone-P and acetyl-CoA (0.5 mM each); and rutin and quercitin (0.1 mM each). Preincubation with 5 mM oxidized glutathione for up to 10 min at 30 °C also had no influence on RcPPC4 activity. Relative to AtPPC3, the activity of the chimeric Class-2 PEPC was significantly less affected by hexose mono-Ps, glycerol 3-P, malate, and Asp (Table 3). These results are reminiscent of analogous comparisons of green algal Class-1 and Class-2 PEPCs (15, 16), as well native Class-1 PEPC and partially degraded Class-2 PEPC (containing proteolytic truncated RcPPC4) from developing COS (10, 13).

The influence of the inhibitor malate on biphasic PEP binding of the Class-2 PEPC was assessed at pH 7.0 (Fig. 6*B*). As the malate concentration increased the contribution of the low $K_{m(PEP)}$ site to the overall activity of Class-2 PEPC was drastically reduced. Catalytic activity from the low K_m site was virtu-

ally absent in the presence of 2 mM malate, such that two distinct activities could not be resolved. The best fit for this curve was to the single catalytic site, Michaelis-Menten model. Conversely, 2 mM malate exerted a negligible effect on the $V_{max(app)}$ of the high K_m site (Fig. 6*B*).

DISCUSSION

Recombinant RcPPC4 Exhibits PEPC Activity—To determine whether *RcPpc4* encodes a functional PEPC, the corresponding cDNA was subcloned into the *E. coli* expression vector pET28b and transformed into the expression strain BL21(DE3). The expressed recombinant RcPPC4 was fully purified from clarified extracts as an active PEPC that exhibited unusual physical and kinetic properties. The specific activity of purified RcPPC4 was 27 units/mg, which compares favorably with that of PEPCs isolated from other plant and algal sources, including the value of 22 units/mg reported for purified recombinant BTPC from the green alga *C. reinhardtii* (20). The high specific activity of RcPPC4 is consistent with the existence in deduced vascular plant BTPC sequences of all conserved subdomains that contribute residues believed to be essential for PEPC catalysis (supplemental Fig. S1) (11, 23). Acetyl-CoA, a potent allosteric activator of many bacterial PEPCs, but not of the vascular plant or green algal enzymes (1), exerted no effect on RcPPC4 activity. Together with the SDS-PAGE and parallel immunoblot analyses shown in Fig. 2 (*panels A* and *B*) this indicates that the purified RcPPC4 was free of any contaminating PEPC originating from the BL21(DE3) host cells. Compared with native and recombinant Class-1 PEPCs (10, 17), RcPPC4 displayed enhanced thermal stability (Fig. 5), an increased $K_{m(PEP)}$ (Table 2), and a noteworthy insensitivity to allosteric effectors. No allosteric activators of RcPPC4 were identified, whereas effective inhibition by malate and Asp only occurred at relatively high concentrations (Table 3). RcPPC4 retains all conserved residues known to bind the effectors malate and Asp, but its insensitivity toward hexose mono-Ps reflects the conspicuous absence in deduced BTPC sequences of two conserved PTPC-specific loops (348–369 and 914–950, maize C_4 PEPC numbering) that are proximal to the Glc-6-P binding site and potentially involved in accommodating the sugar moiety (supplemental Fig. S1) (23, 31, 32).

Recombinant RcPPC4 Forms Class-2 PEPCs When Combined with Class-1 PEPCs—Although COS and green algal BTPCs are catalytically active several independent lines of evidence strongly suggest that the native BTPCs only exist *in vivo* in physical association with corresponding PTPC subunits in a Class-2 PEPC enzyme complex (10, 11, 13–18, 19). It is notable that throughout its purification the recombinant RcPPC4 tends to self-associate into large aggregates of limited solubility, which precluded the use of biophysical techniques for assessing its interaction with Class-1 PEPCs. However, upon mixing freshly prepared *E. coli* extracts containing heterologously expressed RcPPC4 with an excess of recombinant AtPPC3, RcPPC4 was quantitatively bound by AtPPC3 to form a 900-kDa Class-2 PEPC hetero-octameric complex composed of an equivalent ratio of RcPPC4:AtPPC3 subunits (Figs. 1, *B* and *C*; 2, *C*, *D*, and *E*; and 4*E*). All problems pertaining to the insolubility and instability of RcPPC4 during its purification and storage were thereby eliminated, and the chimeric Class-2 PEPC complex never dissociated into its component subunits under non-denaturing conditions. Furthermore, the purified RcPPC4 could only be resolved as a discrete PEPC activity or anti-RcPPC4-IgG immunoreactive band during native PAGE after it was mixed with a Class-1 PEPC (Fig. 4). Native Class-1 PEPCs from developing COS and various vascular plant sources all formed high M_r Class-2 PEPCs when preincubated with the purified RcPPC4 (Fig. 4). The quantitative co-IP of native Class-2 PEPC from clarified COS extracts on an anti-RcPPC4-IgG immunoaffinity column (Fig. 3) corroborated our earlier study that exploited anti-RcPPC3-IgG to co-IP Class-1 and Class-2 PEPCs from developing COS extracts (14). Collective findings of our current and earlier studies support the hypothesis that PTPCs are compulsory and physiologically relevant binding partners for BTPCs that play an indispensable *in vivo* role in maintaining BTPC in its proper structural and functional state in Class-2 PEPCs.

RcPPC4 Functions as a Catalytic and Regulatory Subunit of the Class-2 PEPC Complex—The final specific activity of the chimeric Class-2 PEPC (25 units/mg; Table 1) was more than twice that obtained with the purified native COS Class-2 PEPC containing proteolytically cleaved RcPPC4 (10.3 units/mg) (10). This suggests that the RcPPC4 subunits were catalytically active in the recombinant Class-2 PEPC. Indeed, the recombinant Class-2 PEPC displayed biphasic PEP saturation kinetics (Fig. 6, Table 2) indicating the presence of distinct catalytic sites. This phenomenon was previously documented with the purified non-proteolyzed native Class-2 PEPC from the green alga *S. minutum* in which the high affinity site exhibited $V_{max(app)}$ and $K_{m(PEP)}$ values (7.3 units/mg, 0.13 mM) that were, respectively, about 4- and 10-fold lower than those of the low affinity site (17). These relationships are very similar to those obtained in the current study (Table 2). The high and low $K_{m(PEP)}$ sites of *S. minutum* Class-2 PEPC were attributed to its PTPC and BTPC catalytic subunits, respectively (17). By contrast, three lines of evidence demonstrate that the high and low $K_{m(PEP)}$ sites of the chimeric Class-2 PEPC studied here, respectively, arise from its RcPPC4 (BTPC) and AtPPC3 (PTPC) catalytic subunits: (i) the relevant $K_{m(PEP)}$ values were in the same range as those obtained for the individually purified RcPPC4 and AtPPC3 (Table 2); (ii) 2 mM malate caused a pronounced decrease in the $V_{max(app)}$ of the low, but not high $K_{m(PEP)}$ site (Fig. 6*B*), consistent with purified AtPPC3 exhibiting an $IC_{50(malate)}$ value that was over 60-fold lower than that of the RcPPC4 (Table 3); and (iii) purified native COS Class-2 PEPC containing proteolytically cleaved (inactive) RcPPC4 exhibited classical Michaelis-Menten PEP saturation kinetics with a $K_{m(PEP)}$ of 60 μM at pH 8.0, equivalent to the values determined for the corresponding native RcPPC3 (10), as well as the purified recombinant AtPPC3 examined in the current study (Table 2).

Our kinetic analyses also revealed that the physical interaction between the AtPPC3 and RcPPC4 polypeptides resulted in kinetic activation of both PEPC subunits within the chimeric Class-2 PEPC. It is notable that the $K_{m(PEP)}$ value for AtPPC3 was reduced by about 2-fold upon entering into the Class-2 PEPC complex, whereas that of RcPPC4 decreased by about

one-third (Table 2). The corresponding $V_{max(app)}$ values also appeared to shift. As AtPPC3 and RcPPC4 occur in a 1:1 ratio within the Class-2 PEPC, one can estimate that the $V_{max(app)}$ of its AtPPC3 subunits was actually reduced by about 40% in the complex (from approximately 15 to 9 units/mg of AtPPC3), whereas that of the RcPPC4 subunits was increased by 56% (from approximately 27 to 42 units/mg of RcPPC4) (Table 2). Furthermore, the Class-2 PEPC demonstrated significantly lower sensitivity to allosteric activators (hexose mono-Ps and glycerol 3-P) and inhibitors (malate and Asp) relative to AtPPC3 (Table 3). This agrees with previous studies that have documented the marked insensitivity of native green algal and COS Class-2 PEPC complexes to allosteric effectors, relative to the corresponding Class-1 PEPC (10, 13, 15, 16). Similar to native Class-2 PEPC complexes from green algae and developing COS (10, 15), the chimeric Class-2 PEPC displayed enhanced thermal stability relative to the corresponding Class-1 PEPC (Fig. 5). Results of the present study also corroborate previous work indicating that the tight interaction between RcPPC4 and RcPPC3 subunits in the castor Class-2 PEPC is not influenced by their respective phosphorylation status (13, 14). Nevertheless, *in vitro* dephosphorylation by the catalytic subunit of bovine protein phosphatase type 2A exerted a reciprocal influence on the activity of purified native Class-1 PEPC (inhibited) and partially truncated Class-2 PEPC (activated) from developing COS (13). Determining the influence that *in vivo* multisite BTPC phosphorylation (14) has on the structural and functional properties COS Class-2 PEPC is the subject of ongoing research.

Concluding Remarks—We have provided new insights into the biochemistry of the castor plant BTPC, RcPPC4, and its function as one of two distinct PEPC catalytic subunit types in the unusual Class-2 PEPC enzyme complex of vascular plants. PEPC has been hypothesized to operate at a key branch point in the control of C-partitioning to storage oil and protein in developing seeds. However, it remains to be determined why two distinct oligomeric classes of PEPC are specifically and highly expressed in developing COS. It is apparent that BTPCs readily and tightly bind to Class-1 PEPCs to create unique Class-2 PEPC hetero-oligomers that exhibit altered physical, kinetic, and regulatory properties. The kinetic and regulatory features of the Class-2 PEPC complex are consistent with its putative function as a "metabolic overflow" mechanism that could maintain a significant flux from PEP to malate under physiological conditions that would largely inhibit a Class-1 PEPC. However, we cannot exclude additional functions for Class-2 PEPCs, such as mediating a specific subcellular location and/or further protein-protein interactions (14). It will also be of interest to establish a structural model for plant and algal Class-2 PEPC subunit architecture, and the location of conserved binding domains between their PTPC and BTPC subunits. Patterns of BTPC and Class-2 PEPC expression in various plant species and tissues also need to be re-evaluated together with functional genomic approaches to assess the impact of altered BTPC expression on C-partitioning and carbon-nitrogen interactions in developing seeds.

REFERENCES

1. Chollet, R., Vidal, J., and O'Leary, M. H. (1996) *Annu. Rev. Plant Physiol. Plant Mol. Biol.* **47,** 273–298
2. Izui, K., Matsumura, H., Furumoto, T., and Kai, Y. (2004) *Annu. Rev. Plant Biol.* **55,** 69–84
3. Plaxton, W. C., and Podestá, F. E. (2006) *CRC Crit. Rev. Plant. Sci.* **25,** 159–198
4. Grafahrend-Belau, E., Schreiber, F., Koschützki, D., and Junker, B. H. (2009) *Plant Physiol.* **149,** 585–598
5. Uhrig, R. G., She, Y. M., Leach, C. A., and Plaxton, W. C. (2008) *J. Biol. Chem.* **283,** 29650–29657
6. Xu, W., Ahmed, S., Moriyama, H., and Chollet, R. (2006) *J. Biol. Chem.* **281,** 17238–17245
7. Sánchez, R., and Cejudo, F. J. (2003) *Plant Physiol.* **132,** 949–957
8. Sánchez, R., Flores, A., and Cejudo, F. J. (2006) *Planta* **223,** 901–909
9. Sullivan, S., Jenkins, G. I., and Nimmo, H. G. (2004) *Plant Physiol.* **135,** 2078–2087
10. Blonde, J. D., and Plaxton, W. C. (2003) *J. Biol. Chem.* **278,** 11867–11873
11. Gennidakis, S., Rao, S., Greenham, K., Uhrig, R. G., O'Leary, B., Snedden, W. A., Lu, C., and Plaxton, W. C. (2007) *Plant J.* **52,** 839–849
12. Gousset-Dupont, A., Lebouteiller, B., Monreal, J., Echevarria, C., Pierre, J. N., Hodges, M., and Vidal, J. (2005) *Plant Sci.* **169,** 1096–1101
13. Tripodi, K. E,, Turner, W. L., Gennidakis, S., and Plaxton, W. C. (2005) *Plant Physiol.* **139,** 969–978
14. Uhrig, R. G., O'Leary, B., Spang, H. E., MacDonald, J. A., She, Y. M., and Plaxton, W. C. (2008) *Plant Physiol.* **146,** 1346–1357
15. Rivoal, J., Dunford, R., Plaxton, W. C., and Turpin, D. H. (1996) *Arch. Biochem. Biophys.* **332,** 47–57
16. Rivoal, J., Plaxton, W. C., and Turpin, D. H. (1998) *Biochem. J.* **331,** 201–209
17. Rivoal, J., Trzos, S., Gage, D. A., Plaxton, W. C., and Turpin, D. H. (2001) *J. Biol. Chem.* **276,** 12588–12597
18. Rivoal, J., Turpin, D. H., and Plaxton, W. C. (2002) *Plant Cell Physiol.* **43,** 785–792
19. Moellering, E. R., Ouyang, Y., Mamedov, T. G., and Chollet, R. (2007) *FEBS Lett.* **581,** 4871–4876
20. Mamedov, T. G., Moellering, E. R., and Chollet, R. (2005) *Plant J.* **42,** 832–843
21. Smith, R. G., Gauthier, D. A., Dennis, D. T., and Turpin, D. H. (1992) *Plant Physiol.* **98,** 1233–1238
22. Eastmond, P. J., Dennis, D. T., and Rawsthorne, S. (1997) *Plant Physiol.* **114,** 851–856
23. Kai, Y., Matsumura, H., and Izui, K. (2003) *Arch. Biochem. Biophys.* **414,** 170–179
24. Thomas, J. G., and Baneyx, F. (1997) *Protein Expr. Purif.* **11,** 289–296
25. Kim, M., Elvin, C., Brownlee, A., and Lyons, R. (2007) *Protein Expr. Purif.* **52,** 230–236
26. Plaxton, W. C. (1989) *Eur. J. Biochem.* **181,** 443–451
27. Brooks, S. P. (1992) *BioTechniques* **13,** 906–911
28. Moraes, T. F., and Plaxton, W. C. (2000) *Eur. J. Biochem.* **267,** 4465–4476
29. Gregory, A. L., Hurley, B. A., Tran, H. T., Valentine, A. J., She, Y. M., Knowles, V. L., and Plaxton, W. C. (2009) *Biochem. J.* **420,** 57–65
30. Law, R. D., and Plaxton, W. C. (1997) *Eur. J. Biochem.* **247,** 642–651
31. Takahashi-Terada, A., Kotera, M., Ohshima, K., Furumoto, T., Matsumura, H., Kai, Y., and Izui, K. (2005) *J. Biol. Chem.* **280,** 11798–11806
32. Yuan, J., Sayegh, J., Mendez, J., Sward, L., Sanchez, N., Sanchez, S., Waldrop, G., and Grover, S. (2006) *Photosynth. Res.* **88,** 73–81